Environmental Science & Technology

pubs.acs.org/est

Article

Influence of the Sea Surface Microlayer on Oceanic Iodine Emissions

Liselotte Tinel,* Thomas J. Adams, Lloyd D. J. Hollis, Alice J. M. Bridger, Rosie J. Chance, Martyn W. Ward, Stephen M. Ball, and Lucy J. Carpenter

Cite This: *Environ. Sci. Technol.* 2020, 54, 13228−13237

Read Online

ACCESS | Metrics & More | Article Recommendations | Supporting Information

ABSTRACT: The influence of organic compounds on iodine (I_2) emissions from the $O_3 + I^-$ reaction at the sea surface was investigated in laboratory and modeling studies using artificial solutions, natural subsurface seawater (SSW), and, for the first time, samples of the surface microlayer (SML). Gas-phase I_2 was measured directly above the surface of liquid samples using broadband cavity enhanced absorption spectroscopy. I_2 emissions were consistently lower for artificial seawater (AS) than buffered potassium iodide (KI) solutions. Natural seawater samples showed the strongest reduction of I_2 emissions compared to artificial solutions with equivalent [I^-], and the reduction was more pronounced over SML than SSW. Emissions of volatile organic iodine (VOI) were highest from SML samples but remained a negligible fraction (<1%) of the total iodine flux. Therefore, reduced iodine emissions from natural seawater cannot be explained by chemical losses of I_2 or hypoiodous acid (HOI), leading to VOI. An interfacial model explains this reduction by increased solubility of the I_2 product in the organic-rich interfacial layer of seawater. Our results highlight the importance of using environmentally representative concentrations in studies of the $O_3 + I^-$ reaction and demonstrate the influence the SML exerts on emissions of iodine and potentially other volatile species.

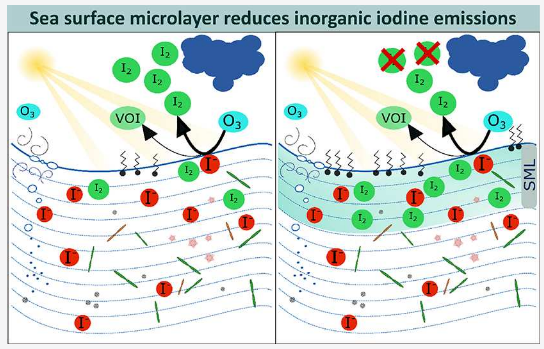

■ INTRODUCTION

Tropospheric iodine is attracting increasing research interest as insights are gained into its large influence on local and global tropospheric and stratospheric chemistry.[1−8] Reactive iodine species, such as IO radicals, induce cycles of catalytic ozone destruction,[5,9,10] change the oxidative capacity of the troposphere through their perturbation of the HOx and NOx cycles,[1,2,11,12] and are linked to particle nucleation.[13,14] Tropospheric iodine levels have tripled since the mid-20th century in certain regions,[15,16] thus a robust understanding of iodine sources into the atmosphere is crucial.

The main source of atmospheric iodine is oceanic emissions.[22] Although biogenic sources contribute to iodine emissions in coastal areas,[17,18] around 80% of atmospheric iodine is believed to arise from abiotic sea-air emissions of inorganic iodine in the form of molecular iodine (I_2) and hypoiodous acid (HOI).[2,19,20] These emissions result from the reaction of ozone with iodide (I^-), which, along with iodate (IO_3^-),[21,22] comprise the main form of oceanic iodine at the sea surface (RR1−RR6)[19,23,24]

$$I^-_{(aq)} + O_{3(g\,or\,aq)} \rightarrow IOOO^- \quad (R1)$$

$$IOOO^- \rightarrow IO^-_{(aq)} + O_2 \quad (R2)$$

$$IO^-_{(aq)} + H^+ \rightarrow HOI_{(aq)} \quad (R3)$$

$$HOI_{(aq)} + I^- + H^+ \rightleftharpoons I_{2(aq)} + H_2O \quad (R4)$$

$$I_{2(aq)} \rightleftharpoons I_{2(g)} \quad (R5)$$

$$HOI_{(aq)} \rightleftharpoons HOI_{(g)} \quad (R6)$$

On average, the global sea surface iodide concentration (upper 20 m) is estimated at 9.5×10^{-8} M.[25] Typical iodine sea-air fluxes calculated for the clean marine boundary layer lie in the range of 100−250 nmol m^{-2} d^{-1} for HOI and 2−10 nmol m^{-2} d^{-1} for I_2.[19,26]

Iodide reacts very rapidly with ozone (RR1), much faster than the equivalent reactions of Cl^- and Br^- ($k_{I-} = 2 \times 10^9$ M^{-1} s^{-1}, $k_{Br-} = 1{-}2 \times 10^3$ M^{-1} s^{-1}, $k_{Cl-} \sim 3 \times 10^{-3}$ M^{-1} s^{-1}), explaining the major influence iodide has on the dry deposition of ozone, despite its much smaller concentration in seawater ([Cl^-] = 5.6×10^{-1} M; [Br^-] = 8.6×10^{-4} M).[27−30] The fast reactivity of iodide with O_3 and its enhancement at the air−water interface[31,32] suggests that heterogeneous surface reactions would be promoted. However, at low iodide

Received: April 30, 2020
Revised: September 23, 2020
Accepted: September 25, 2020
Published: September 25, 2020

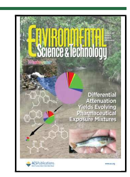

conditions ($[I^-] < 10^{-5}$ M) such as found at the sea surface, the reaction is dominated by aqueous-phase bulk reactivity for all atmospherically relevant ozone concentrations.[33] This is explained by the relatively high reacto-diffusive length (a few micrometers) as a result of a slow rate of O_3 consumption under these low $[I^-]$, natural conditions.[33]

The influence of organic compounds on the ozone + iodide reaction remains unclear. Due to the presence of other ions and virtually unknown quantities of various dissolved organics, the sea surface is a chemically complex, but dilute, system. The surface microlayer (SML), the uppermost 1 to 1000 μm of the sea surface, represents a less dilute environment where surface-active organics can become significantly enriched.[34,35] By its nature, the SML constitutes the interface between the air and water, and its influence on air-sea exchange has been demonstrated for trace gases, e.g., CO_2[36] and N_2O.[37] However, the underlying mechanisms remain largely unknown and it is not clear to what extent the presence of natural surfactants modifies oceanic gaseous emissions.[38,39]

Organics influence iodine emissions in different ways via several mechanisms, as summarized in Table S1. A suppression of I_2 emissions was observed in the presence of a monolayer of octanol,[40] whereas short-chain carboxylic and fulvic acids enhanced I_2 emissions.[41] Chemical competition for O_3 by phenolate ions at the surface also suppresses I_2 emissions.[42] The addition of a complex organic matrix, dissolved organic carbon (DOC) extracted from natural seawater, to buffered solutions of iodide has been found to lead to a strong reduction of $I_{2(g)}$ emissions.[43] This reduction could not be explained by the reactivity of DOC toward O_3 and I_2/HOI, and instead a decrease in the net transfer rate of I_2 from the aqueous to gas phase was suggested,[43] as previously observed for octanol.[40] Conversely, ozonolysis of coastal seawater samples can generate certain halocarbons (CH_2I_2, CHI_3, and $CHClI_2$),[44] implying that reactions of the I_2 (or HOI) product in solution can yield organic iodine species. However, no direct link has been demonstrated between the emission of halocarbons and the presence of dissolved organics or reduced emission of inorganic iodine. Overall, these studies show that introducing a single organic component can alter iodine emissions through chemical enhancement, suppression, and/or physical hindrance.

Here, we compare iodine ($I_{2(g)}$) emissions from the dark reaction of ozone with iodide in buffered potassium iodide solutions and artificial seawater (AS), against natural subsurface seawater (SSW) and, for the first time, SML samples. Importantly, these experiments were performed for ozone mixing ratios (20−150 ppbv) and iodide concentrations (1×10^{-7} to 1.6×10^{-5} M), which include ambient conditions. The dependence on ozone and iodide concentrations is investigated and the influence of organic materials is discussed. In separate experiments, we explore halocarbon production from the ozone + iodide reaction, comparing halocarbon emissions from artificial seawater, SSW and SML samples, as functions of ozone and iodide concentrations. The implications of these first I_2 and organic emission measurements using natural SML samples are explored using an adaptation of the aqueous interfacial layer model of Carpenter et al.[19]

■ MATERIALS AND METHODS

Chemicals. Buffered solutions of iodide were prepared by adding concentrated KI stock solutions to a phosphate buffer at pH 8. Artificial seawater (AS) solutions were made by dissolving KCl and KBr in a phosphate buffer and then adding aliquots of the KI stock solutions. Full details are in the Supporting Information (SI).

Sampling and Analysis of Seawater. The samples of natural seawater were obtained from the North Sea, 5 km off-shore from Bridlington (U.K.), and filtered through GF/F ashed quartz filters. Iodide in the samples was measured using cathodic stripping voltammetry. DOC was determined using a total organic carbon analyzer. Surface tension was measured using the DuNoüy ring method. Details about the sampling locations, dates, procedures, and methods can be found in SI, Sections S1.2−S1.5 and Table S2.

In Situ I_2 Measurements. Figure S1 shows the apparatus for in situ measurements of molecular iodine by broadband cavity enhanced absorption spectroscopy (BBCEAS). A 250 cm^3 min^{-1} flow of synthetic air (BTCA-178, BOC special gases) passed through an ozone generator and mixed with 3500 cm^3 min^{-1} of synthetic air before entering the custom-built glass reaction vessel. The vessel contained 500 cm^3 of aqueous solution with a surface area of approx. 380 cm^2, leaving a headspace of 4800 cm^3 where the BBCEAS light beam was integrated. Iodine concentrations were measured approximately 3.5 cm above the liquid's surface. Two additional air flows, 200 cm^3 min^{-1} in total, were used to purge the cavity mirrors; thus, the total flow through the vessel was 3950 cm^3 min^{-1}. The vessel was thermostatted and covered in aluminum foil to avoid photolytic losses of I_2 (or the production of IO radicals). The solution was actively stirred at the same rate for all experiments by means of a central magnetic stirrer, and solutions were brought to temperature before introduction into the vessel. Experiments recorded I_2 emissions versus increasing iodide concentrations by adding aliquots ($\sim$1 cm^3) of concentrated potassium iodide solutions (1×10^{-4} or 1×10^{-3} M) to the sample solutions through a lid at the top of the vessel.

Retrieving I_2 concentrations followed a similar procedure to previous BBCEAS measurements.[45] Further details appear in the SI. The errors reported include the statistical uncertainty of the spectral fit, dominant at small concentrations, and the systematic errors of the measurement (typically totaling 16% for I_2, see the SI). The limit of detection for iodine (LoD) was 4 pptv (1 σ in 60 s), which corresponds to a minimum detectable I_2 flux of 1.5×10^7 molecules cm^{-2} s^{-1}. All iodine data was corrected for losses in the reaction vessel due to the gas-phase reaction of $I_2 + O_3$ using the rate constant $k_{(I_2 + O_3)} = 2.25 \times 10^3$ M^{-1} s^{-1}.[46] These losses proved to be negligible (<1% of the I_2 emissions) for the low reactant concentrations of our experiments and the relatively short residence time of gas inside the reactor (73 s).

Ozone, measured using commercial UV absorbance ozone monitors, was monitored upstream and downstream of the vessel by switching a three-way valve. O_3 measurements are detailed in the SI. All results presented here were obtained for solutions and seawater samples at 17 °C.

Halocarbon Measurements. The production of halocarbons was examined using the setup depicted in Figure S2. The system was designed to flow 500 cm^3 min^{-1} of dry hydrocarbon-free air through a mass flow controller, with or without ozone, into the reaction vessel (500 cm^3 round-bottom glass flask). There, it passed over 250 cm^3 of degassed artificial seawater or natural samples (surface area of 105.7 cm^2) before sampling. The entire reaction vessel and tubing

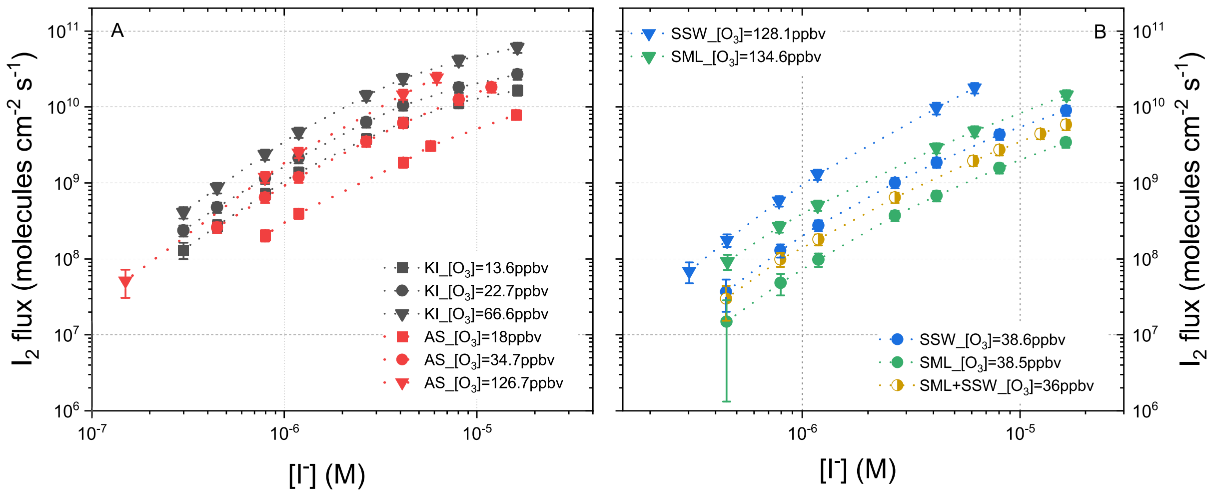

Figure 1. Panel A: BBCEAS measurements of I_2 emissions as a function of $[I^-]$ over buffered KI solutions (black points) for ozone concentrations of 13.6 ppbv (squares), 22.7 ppbv (circles), and 66.6 ppbv (triangles) at 17 °C. The red symbols are the I_2 emissions over artificial seawater for $[O_3]$ = 18 ppbv (squares), 34.7 ppbv (circles), and 126.7 ppbv (triangles). Panel B: BBCEAS measurements of I_2 emitted from the natural samples of subsurface seawater (blue, SSW), surface microlayer (green, SML), and a mixture of 20% SML + 80% SSW (gold) for ozone concentrations of 38.6, 38.5, and 36 ppbv, respectively (circles). The triangular symbols show I_2 recorded at higher ozone concentrations over SSW ($[O_3]$ = 128.1 ppbv) and SML ($[O_3]$ = 134.6 ppbv). All measurements at 17 °C. The dotted lines are the straight segments between the points, meant to guide the eye. The error bars reflect the overall uncertainty on the measurements, including the uncertainty on the spectral fit, averaging and systematic errors.

were thermostatted and covered in aluminum foil to prevent halocarbon losses due to wall losses and photolysis. During all experiments, the solution was gently stirred using a magnetic stirrer to avoid depletion at the surface and to mimic the dynamics at the sea surface. The halocarbon products were trapped using an air server coupled to a thermal desorption unit (CIA-8, Unity-2, Markes, U.K.) and then analyzed using gas chromatography coupled to a mass spectrometer (GC−MS, Agilent 6890, 5975C). Further details are in the SI.

Modeled Iodine Emissions: The Sea Surface Model. The interfacial model described in Carpenter et al.[19] was used, with some modifications, to estimate I_2 (and HOI) emissions from this study's experiments. Full details can be found in the SI. Briefly, we assumed that the ozone uptake coefficient γ_{I^-} is controlled by the aqueous-phase $O_3 + I^-$ reaction and is equivalent to γ_{aq,I^-}, with

$$\frac{1}{\gamma_{aq}^{I^-}} = \frac{1}{\alpha_{aq}^{I^-}} + \frac{1}{\Gamma_{aq}^{I^-}} \tag{1}$$

where α_{aq}^{I-} is the mass accommodation coefficient and Γ_{aq}^{I-} is the conductance of the aqueous-phase reaction, given by

$$\Gamma_{aq}^{I^-} = \frac{4s\sqrt{k^{I^-} \times a_{I^-} \times D_{aq}}}{\omega} \tag{2}$$

In eq 2, s is the ozone solubility in nondimensional units (aqueous molarity/gas molarity), k^{I-} is the rate constant for the aqueous-phase reaction $O_3 + I^-$, a_{I^-} is the activity of iodide, and D_{aq} is the diffusion coefficient of aqueous ozone. The values of s and D_{aq} were calculated according to the salt content of the water.[33,47−49]

At the higher iodide conditions of our experiments ($[I^-] > \sim 1 \times 10^{-5}$ M), surface reactions may add an appreciable extra component to O_3 uptake (e.g., refs 33, 50). In the SI, we describe a sensitivity study where we included total surface and bulk phase O_3 uptake in the model,[50] without any changes to the iodine emissions scheme. Noting that the model is designed to simulate environmental conditions where the aqueous reaction dominates ($[I^-] < 1 \times 10^{-5}$ M), and that those are the experimental conditions used here, we did not include surface reactivity for the remainder of this work.

Rapid production of $I_{2(aq)}$ follows the reaction of iodide at the aqueous surface with O_3 deposited from the gas phase (RR1−RR4). The aqueous iodine reaction scheme used here was the same as in Carpenter et al.[19] except for a modification to reflect that $I_{2(g)}$ emissions observed from artificial seawater (AS) were only around 50% of those from buffered potassium iodide solutions. The reasons for this are unknown, but a potential explanation could be a competing oxidation of HOI to iodate (IO_3^-) by $HOCl/OCl^-$ or $HOBr/OBr^-$,[51] formed through heterogeneous reactions of Cl^- and Br^- with O_3.[52,53] It is beyond the scope of this study to attempt to model such chemistry explicitly. Rather, we included the reactions HOI + $HOCl/OCl^- \rightarrow IO_3^-$ as a proxy for the reduction of iodine emissions observed in the presence of Cl^- or Br^-. An assumed total of 2 mM of $HOCl/OCl^-$ (for seawater concentrations of Cl^- and Br^-; 54% of deprotonated HOCl at pH = 8) was sufficient to dampen modeled I_2 emissions by ∼50% in artificial seawater compared to equivalent conditions over KI solutions. We included this $HOCl/OCl^-$ reaction in all simulations of natural or artificial seawater.

Concentrations of $[I^-]$, $[H^+]$, and $[OH^-]$ were fixed for each model run. For modeling iodine emissions from SSW and SML, we included (as in ref 19) pseudo-first-order rate constants for "O_3 + DOC" interfacial reactions of 100 s^{-1} and for "I_2/HOI + DOC" of 7×10^{-3} s^{-1}.[6,54] We also utilized the latter reaction to explore the potential for volatile organic iodine production.

EXPERIMENTAL RESULTS AND DISCUSSION

Molecular Iodine (I_2) Emissions. The influence of organics in solution on gaseous inorganic iodine emissions was investigated using BBCEAS to monitor I_2 emitted from the ozonolysis of buffered solutions of KI, artificial seawater (AS),

https://dx.doi.org/10.1021/acs.est.0c02736
Environ. Sci. Technol. 2020, 54, 13228−13237

natural subsurface seawater (SSW), and sea surface microlayer (SML) samples.

Artificial Solutions. Figure 1, panel A, shows that iodine emissions were readily detected from KI solutions, even for low ozone and the lowest iodide concentrations tested (3×10^{-7} M). Increasing iodide concentrations led to higher concentrations of gas-phase I_2 under all experimental conditions. Emissions increased almost linearly with increasing ozone and increasing [I^-], although some roll-off in linearity was observed for the highest iodide concentrations ($\geq 8 \times 10^{-6}$ M).

I_2 production over artificial seawater (AS, Figure 1A) shows a very similar trend, but with overall lower I_2 flux rates than for KI solutions. Over AS, the lowest iodide concentration [I^-] = 1.5×10^{-7} M and lowest ozone concentration (17 ppbv) did not produce I_2 emissions above the detection limit of the BBCEAS system. For all other ozone concentrations (35−127 ppbv) and iodide concentrations, I_2 was detected above the LoD, showing a generally linear increase with [O_3].

The fluxes obtained in our experiments with KI solutions correspond well to previous observations. Carpenter et al.[19] reported a flux $I_{2\ \mathrm{emitted}} = 4 \times 10^{10}$ molecules cm^{-2} s^{-1} for a buffered iodide solution with [I^-] = 1.5×10^{-5} M and [O_3] = 35 ppbv at 20°C. Under similar conditions, [I^-] = 1.6×10^{-5} M and [O_3] = 37.2 ppbv at 17 °C, the flux observed in this study is slightly lower, $I_{2\ \mathrm{emitted}} = 3.3 \times 10^{10}$ molecules cm^{-2} s^{-1}. The observed I_2 fluxes also agree well with observations reported in MacDonald et al., from solutions without chloride.[55] The flux observed here, for [I^-] = 1.2×10^{-6} M and [O_3] = 66.6 ppbv, is $I_{2\ \mathrm{emitted}} = 4.6 \times 10^9$ molecules cm^{-2} s^{-1}. This compares well with their $I_{2\ \mathrm{emitted}} = 4.9 \times 10^9$ molecules cm^{-2} s^{-1} for a buffered solution of [I^-] = 1×10^{-6} M and [O_3] = 78 ppbv.[55]

When comparing I_2 fluxes over artificial seawater, our observations are about 3 times smaller than in MacDonald et al.[55] using a similar chloride concentration (0.5 M) for [I^-] = 1×10^{-6} M. MacDonald et al.[55] report an I_2 flux of 12×10^9 molecules cm^{-2} s^{-1}, whereas the flux calculated by extrapolating our AS data to the same ozone concentration (222 ppbv) is around 3.9×10^9 molecules cm^{-2} s^{-1}. However, there are some important differences that may explain this discrepancy. First, MacDonald et al. did not stir the liquid phase for their experiments, a condition known to lead to higher emissions due to reduced downmixing of products formed, making unstirred conditions less representative of the turbulent surface layer of the ocean.[19] Second, the AS used here contains bromide, whereas the MacDonald study used only chloride. Although the reaction of bromide with ozone is slow as stated in the introduction, bromide reacts quickly with HOI to form BrI ($k = 4.1 \times 10^{12}$ M^{-1} s^{-1}), which could further contribute to the lower emissions observed here.[56]

The I_2 emissions observed over buffered KI solutions showed a near linear increase with increasing ozone concentrations (Figure 2, black squares). Although nonlinear behavior of I_2 emissions as a function of ozone has been observed under high iodide (5×10^{-3} M) and high ozone conditions (over ∼100 ppmv), linear behavior in ozone is expected for our iodide and/or ozone concentrations or lower.[19,24] At conditions representative for the open ocean's surface (low ozone, low iodide), I_2 emissions can thus be expected to scale linearly with [O_3] as also predicted by the interfacial model (see section: Interfacial Model Results and Discussion). Figure 2 shows that lower I_2 emissions were observed when using artificial seawater solutions compared to

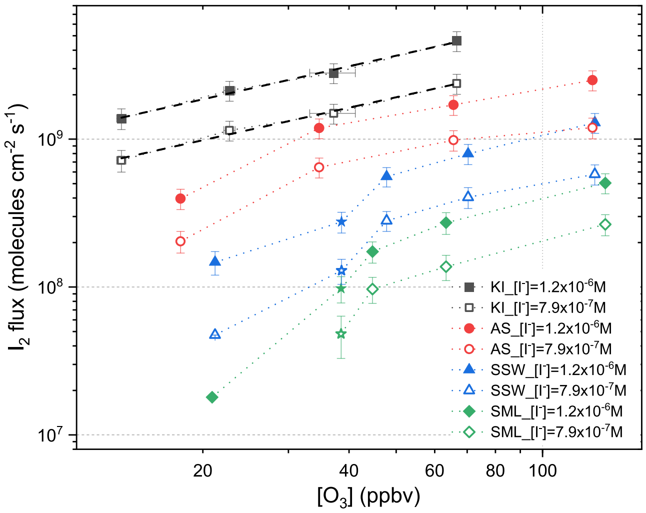

Figure 2. Measured I_2 emissions at 17 °C as a function of ozone concentration for total [I^-] = 1.2×10^{-6} M (filled symbols) and total [I^-] = 7.9×10^{-7} M (open symbols) over buffered KI solutions (black squares), artificial seawater (red circles), subsurface seawater (blue triangles), and surface microlayer sample (green diamonds). The I_2 measurements from SSW and SML used samples collected on 04/05/2018, except measurements at [O_3] = 38.6 ppbv, which were done with the samples collected on 15/08/2018, as indicated by the star symbol on the graph (see Table S2 for more details); variability in the organic content of the natural SSW and SML samples might explain why the I_2 emissions recorded at 38.6 ppbv O_3 lie below the trend of the data points at other O_3 concentrations. The dotted lines are straight segments that join the data points, meant to guide the eye. The heavy dashed black lines through the buffered KI data points are linear regressions ($y = 8.36 + 0.69x$ and $R^2 = 0.94$ for [I^-] = 1.2×10^{-6} M; $y = 8.09 + 0.68x$ and $R^2 = 0.93$ for [I^-] = 7.9×10^{-7} M). The error bars reflect the overall uncertainty on the measurements, including the uncertainty on the spectral fit, averaging and systematic errors.

buffered KI solutions at all ozone concentrations. Since the only change between the experiments with the buffered KI solutions and artificial seawater is the addition of potassium chloride and bromide, this change in salinity seems to provoke the observed change in emissions.

Several factors could contribute in explaining the reduction in I_2 emissions from AS compared to buffered KI solutions. Magi et al.[27] estimated that O_3 diffusivity decreases by 12% in a 3 M sodium iodide solution compared to pure water, but the resulting effect on the uptake of ozone (<6%) is negligible compared to the 3× differences we observed between KI and AS at our much lower salt concentrations. Based on these results and because diffusivity is difficult to predict, changes in diffusivity are generally ruled out as an important factor in the uptake of ozone.[33] However, it is well documented that increased salinity almost always decreases the solubility of gases through the so-called "salting-out effect".[57] We calculated the solubility of ozone under our experimental conditions at 17 °C for KI and AS solutions following the approach in Moreno et al.[33] For the highest iodide concentration used here ([I^-] = 1.6×10^{-5} M), the calculated solubility of ozone is 1.15×10^{-7} M atm^{-1} in a solution of KI and 1.01×10^{-7} M atm^{-1} in AS, representing a decrease of 12%. This higher solubility of ozone in a solution of KI compared to AS alone cannot explain our observed differences in I_2 emissions. Additional reactions of ozone with Br^- and Cl^- could become important at ozone concentrations substantially above what

https://dx.doi.org/10.1021/acs.est.0c02736
Environ. Sci. Technol. 2020, 54, 13228−13237

our study used, although the interfacial model does not predict this nonlinear behavior for I_2 emissions. Other reasons for the reduced I_2 emissions from AS compared with buffered KI solutions will be explored in detail in the model result section.

Natural Seawater Samples. Substantial reductions in I_2 emissions were observed over subsurface seawater and surface microlayer samples compared to AS and KI solutions. This confirms the reduction of iodine emissions in the presence of organics reported in previous studies of the reaction of ozone with iodide[19,40,43] and shows, for the first time, a further reduction over SML samples. Figure 2 compares emissions observed over all four types of solution as a function of $[I^-]$. Two different samples were used for these experiments, as indicated by the star symbol in Figure 2 (further details in Table S2). For all ozone concentrations (20−145 ppbv), I_2 was below the BBCEAS detection limit over SSW or SML (containing natural $[I^-]$ of 1.04 to 1.53 × 10^{-7} M, see Table S2). However, I_2 was detected from SSW and SML after the addition of relatively small amounts of iodide ($[I^-]_{total} \geq 2.98 \times 10^{-7}$ M, i.e., approximately double the naturally occurring $[I^-]$), even at 38 ppbv ozone (typical of mid-ocean ambient O_3 concentrations).

Figures 2 and 1B both clearly show that I_2 emissions over SML samples are lower than those over SSW samples by an average of 65 ± 4% (and by up to a maximum of 83%), and the reduction is similar for both sampling dates (Figure S3). A further experiment at $[O_3]$ = 36 ppbv with a mixture of SML/SSW (20/80 by volume; gold symbols in Figure 1B) showed I_2 emission intermediate between the "pure" SSW and SML results. Interestingly, the I_2 fluxes from this mixed sample were 38% lower (averaged over all $[I^-]$ data) than the emissions expected from a simple 20:80 weighted average of the emissions from pure SML and pure SSW, which could indicate that organics from the minor SML component preferentially partitioned to the air−liquid interface where I_2 emissions are more efficiently suppressed. As discussed later, we attribute the substantially decreased emissions from the SML compared to the SSW to the enrichment of organics in the SML. However, I_2 emissions from different sets of the SML/SSW samples did not necessarily show the expected relationships with the presence of organics. For example, the SML and SSW samples from 15/08/18 (Table S2) had lower [DOC] and higher surface tension than the SML sample from 04/05/18, yet showed approximately 63% lower emission over SML compared to SSW collected on the same day. Detailed chemical analysis of a large number of SML and SSW samples (preferably collected from different geographical locations), which is beyond the scope of this present study, would be required to identify groups or individual compounds most involved in this reduction.

Similar to the artificial solutions, increasing ozone concentrations over natural seawater samples led to higher I_2 emissions (Figure 2) in a generally linear trend. The emissions from SSW with $[O_3]$ = 38.6 ppbv seem to be lower than the general trend observed across the other ozone concentrations, but this sample was collected on a different date (15/08/18) than the samples used to determine I_2 emissions from other ozone concentrations (04/05/18), which might explain the difference observed. More observations over natural samples are needed to further disentangle the relation between particular types of DOC, surface tension, and their effects to reduce I_2 emissions.

Halocarbon Emissions over Artificial and Natural Seawater. A separate set of experiments monitored emissions of halocarbons from the reaction of ozone at the surface of artificial solutions (buffered KI solution and AS) and natural samples (SSW, SML). Although no organic material was added, some production of halocarbons was observed upon the ozonolysis of artificial solutions, despite having purged the solution with N_2. Without ozone, the emissions were close to or below the LoD, and therefore these zero ozone experiments were used as blanks. For the natural seawater samples, halocarbon emissions without ozone were mostly below the LoD, and where they were above, they were an order of magnitude smaller than with ozone.

The most abundant halocarbon produced from exposing natural and artificial samples to ozone was methyl iodide (CH_3I); this was the only volatile organic iodine (VOI) compound that was consistently emitted. Other halocarbons observed above their LoDs were CH_2ClI, C_2H_5I, 1-C_3H_7I, 2-C_3H_7I, $CHBr_2Cl$, and CH_2Br_2, although the latter two were only observed for the highest ozone concentrations (1 ppmv) over natural samples. The summed total of these compounds represents less than 10% of the total VOI flux; the other >90% is CH_3I. The 11 different volatile organic iodine compounds monitored (see Section S1.8 and Table S3 in the SI) were not all emitted from all 4 types of solutions, and different compounds showed different trends for KI, AS, SSW, and SML. But overall, the highest VOI emissions were seen when ozone reacted with the SML samples and increased with increasing ozone. CH_2I_2 and CH_2BrI were not observed above their LoDs and, due to a high background, $CHBr_3$ was not significantly observed either.

Due to the complexity of the product distribution and the small flux for each compound individually, we focus only on the summed total of the VOI. Figure 3 shows the VOI emissions measured over the four different types of solutions for two ozone concentrations, both substantially above

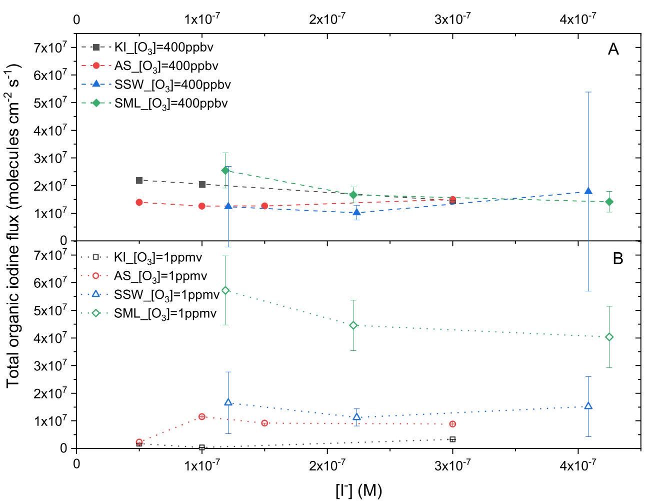

Figure 3. Measured total volatile organic iodine emissions as a function of iodide concentration over buffered KI solution (black squares), artificial seawater (red circles), subsurface seawater (blue triangles), and surface microlayer (green diamonds) samples at 20 °C for (A) $[O_3]$= 400 ppbv (filled symbols) and (B) $[O_3]$= 1 ppmv. The dotted lines are straight segments between the points, meant to guide the eye. The error bars reflect the uncertainty on the quantification of the halocarbons.

https://dx.doi.org/10.1021/acs.est.0c02736
Environ. Sci. Technol. 2020, 54, 13228−13237

ambient $[O_3]$, but at iodide concentrations relevant for ambient seawater. The VOI emissions show no clear trend with increasing iodide concentrations. The emissions after exposure to 400 ppbv of ozone (Figure 3A) are rather similar for the different solutions. However, VOI emissions are clearly higher for the 1 ppmv ozone experiments over the natural samples, particularly SML (Figure 3B). A maximum flux of $VOI_{\text{emitted}} = 5.7 \times 10^7$ molecules cm^{-2} s^{-1} was measured over the SML sample exposed to 1 ppmv of ozone with $[I^-] = 1.2 \times 10^{-7}$ M (i.e., without adding further iodide). Nevertheless, this peak VOI flux is still small compared to the inorganic I_2 fluxes reported in the previous sections, where much lower ozone concentrations were used. For example, a comparable flux of iodine of $I_{\text{emitted}} = 3.0 \times 10^7$ atoms cm^{-2} s^{-1} (due to $I_{2\,\text{emitted}} = 1.5 \times 10^7$ molecules cm^{-2} s^{-1}) was observed over a surface microlayer sample with $[I^-] = 4.5 \times 10^{-7}$ M exposed to only 38.5 ppbv of ozone (Figure 1). Clearly, the VOI flux will represent only a small fraction of the total iodine flux at environmentally relevant ozone concentrations. Using the interfacial model to estimate emission fluxes at $[O_3] = 400$ ppbv over SML with $[I^-] = 1$ to 4.3×10^{-7} M, we calculate $I_{2\,\text{emitted}} = 50$ to 193×10^7 molecules cm^{-2} s^{-1} and $HOI_{\text{emitted}} = 2.2$ to 8.3×10^9 molecules cm^{-2} s^{-1}. Correspondingly, the observed VOI fluxes from SML for 400 ppbv O_3 (1.5 to 2.6×10^7 atoms cm^{-2} s^{-1} in Figure 3A) represent between 2.5 and 0.4% of the emissions of iodine atoms from I_2 and VOI and only 0.1 to 0.8% of the total iodine flux (VOI + 2 × I_2 + HOI). Thus, we conclude that VOI emissions make a negligible contribution to the total iodine flux.

Interfacial Model Results and Discussion. Figure 4 shows a comparison of the model results and I_2 emissions observed from the four different types of solutions used in this study at atmospherically relevant ozone concentrations.

Artificial Solutions. The interfacial model was first used to predict iodine emissions over buffered KI solutions, and the full dataset is shown in Figure S4A. The model captures the trends of I_2 emissions with O_3 and with I^- well, although it tends to underestimate the iodine flux at low $[O_3]$.

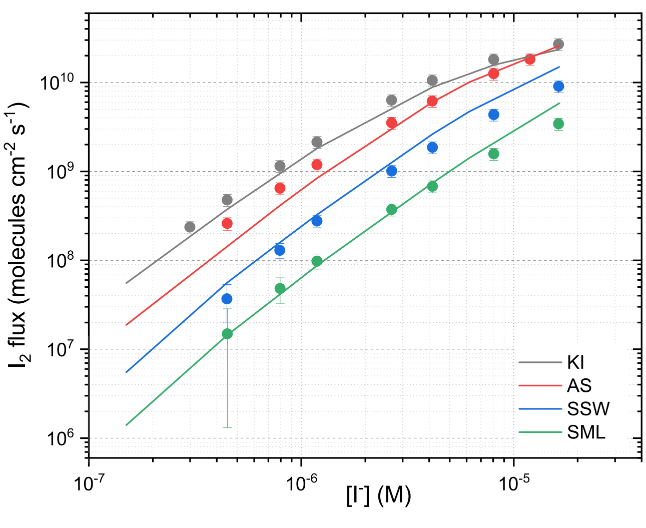

Figure 4. Observations (symbols) and modeling (lines) of I_2 emissions at 17 °C as a function of I^- concentration from buffered KI solutions (gray), artificial seawater (red), subsurface seawater (green), and surface microlayer (blue) for ozone concentrations of 22.7, 34.7, 38.6, and 38.5 ppbv, respectively. The error bars reflect the overall uncertainty on the measurements. The plot extends the calculation of the modeled I_2 emissions back to an iodide concentration of 1.5×10^{-7} M, typical of natural oceanic surface iodide concentrations.

Modeled emissions over artificial seawater are compared to the observations in Figure S4B. Note that, as discussed in the methods section, a completing oxidation reaction of HOI (to iodate) by $HOCl/OCl^-$ was incorporated into the model to account for the ~50% decrease in I_2 emissions observed in AS compared to equivalent KI solutions. Although the model somewhat underpredicts I_2 emitted at low O_3, overall the model shows skill in matching the observations. The experimental emissions for the lowest $[I^-]$ (black points, Figure S4) are close to the LoD, yet the modeled I_2 flux falls within the observational uncertainty.

Natural Seawater Samples. As detailed in the experimental results section, a substantial reduction in iodine emissions was observed from natural samples compared to artificial seawater and KI solutions. Previous studies on the reaction of gas-phase ozone with iodide solutions have established that I_2 emissions are reduced in the presence of organics.[19,40,43] All of these studies attributed the reduction to a suppression of the liquid–gas transfer rate of I_2. Shaw and Carpenter[43] found that emissions were increasingly suppressed by DOC, by up to a factor of two, at ratios of [DOC]:[iodide] representative of their ambient reactivities to $O_3(g)$. Qualitatively, this is consistent with the reduction we observed in the SSW samples.

Using the same (but unmodified) interfacial model as we use in this study, Shaw and Carpenter[43] showed that neither DOC competing with I^- to react with interfacial O_3 nor direct loss of I_2 and/or HOI through reaction with DOC could fully explain the reduction of I_2 emissions from SSW. Instead, they proposed a reduction in the net liquid–gas transfer rate of I_2 in SSW. Nevertheless, the reduction of the I_2 liquid–gas transfer rate is a hypothesis that has hitherto not been explored in detail. Iodine (I_2) is a nonpolar molecule and is many times more soluble in organic solution than in water; for example, iodine has an octanol–water partition coefficient K_{OW} of 309.[58] An estimate of the octanol–air partition coefficient (K_{OA}) of I_2 can be made by assuming $K_{OA} = K_{OW}/K_{AW}$, where K_{AW} is the air–water partition coefficient for I_2.[59] Translated into the equations for mass transfer of I_2 under our laboratory conditions, the liquid–air mass transfer K_T of I_2 from a pure octanol monolayer would be reduced by a factor of 99.3 compared to that from a purely aqueous solution at room temperature. We found that reducing the model's aqueous–air mass transfer term of I_2 at 17 °C from 1.04×10^{-6} to 4×10^{-7} s^{-1} (i.e., ~40% of the pure water transfer term) produced a good agreement between the model and the SSW observations (see Figure S5A and further details in section 1.9 of the SI). Thus, assuming that the reduction in I_2 emissions was entirely due to its increased solubility in the more organic-rich seawater than in pure water, this equates to an enhancement of I_2 solubility in seawater of about a factor of 6 (i.e., to ~0.2 g/kg at 20 °C) compared to its value in pure water (0.03 g kg^{-1} at 20 °C). Note that, while changes in solubility can explain the mass transfer of iodine under the still, laboratory conditions of the experiments presented here, additional factors caused by surfactants, such as, e.g., physical suppression of near surface mixing, might influence emissions under real-world conditions.

To explore the role of chemistry in reducing the I_2 emissions, we modeled the loss of I_2 and HOI through their reactions with DOC, as described in Materials and Methods. Including such chemistry had a negligible (<2%) impact on the

https://dx.doi.org/10.1021/acs.est.0c02736
Environ. Sci. Technol. 2020, 54, 13228−13237

I_2 emissions from SSW. This result strengthens our conclusion that I_2 emissions are reduced in seawater compared to artificial seawater due to the enhanced solubility of I_2, rather than by its chemical loss.

I_2 emissions from SML samples were typically a factor of 3–4 times lower than from subsurface seawater. The SML I_2 emissions were modeled satisfactorily, as shown in Figure S5B, by further reducing the aqueous–air mass transfer term for I_2 to 1×10^{-7} s^{-1} (i.e., now only 10% of the pure water transfer term). This corresponds to the solubility of I_2 in the SML being around 5 times higher than in SSW, at around 1 g kg^{-1} at 20 °C.

Figure 4 shows how the model performs well to predict iodine emissions from the natural samples over iodide concentrations up to 4×10^{-6} M for ambient ozone conditions. As the concentration of iodide in the open seawater generally ranges between 10 and 150×10^{-9} M,[25] this interfacial model can be a useful tool for predicting marine iodine emissions.

Volatile Organic Iodine Emissions. I_2 and HOI reactions with DOC were included in the model to explore whether such chemistry could broadly explain the VOI emissions from the SML following the $O_{3(g)} + I^-_{(aq)}$ reaction. We assumed a pseudo-first-order rate constant for the reaction of I_2 and HOI with DOC of 7×10^{-3} s^{-1} (see Materials and Methods), a 100% yield of VOI products (initially), and that VOI that is mixed downward out of the reacto-diffusive depth layer into the bulk is irreversibly lost, equivalently to I_2 and HOI. This gives a lower limit to the potential VOI emissions, since, unlike I_2 and HOI that react rapidly away in the bulk waters, some fraction of VOI molecules mixed down from the surface will persist long enough to be re-emitted. Nevertheless, this simple scenario produced VOI emissions an order of magnitude greater than we observed. However, it is known that reduction of I_2 and HOI emissions by DOC also leads to the formation of dissolved organic iodine (DOI), which was not monitored in our experiments, and reforms I^- (e.g., ref 54, 60). We found that setting the VOI yield (from reaction of I_2 and HOI with DOC) to 5–10% gave the correct order of magnitude for the VOI emissions (1 to 4×10^7 molecules cm^{-2} s^{-1} total VOI for $[I^-]$ between 1 and 4×10^{-7} M, Figure S6) and VOI fluxes scaled with the gaseous O_3 concentration, as found experimentally (previous section, Figure 3). However, the model predicted an increase in VOI emissions as $[I^-]$ increased from 1 to 4×10^{-7} M, whereas the observed VOI emissions from the SML in Figure 3 actually declined; modeled VOI emissions only decline above $[I^-] > \sim 1 \times 10^{-5}$ M (Figure S6). Modeled VOI emissions as a fraction of the total iodine emissions (VOI + 2 × I_2 + HOI) decreased strongly with increasing $[I^-]$, which is likely due to the $I_2 + I^-$ reaction competing with I_2 + DOC as $[I^-]$ increases.

Environmental Implications. Our experiments show a clear reduction of molecular iodine emissions from the $O_{3(g)} + I^-_{(aq)}$ reaction in seawater (compared to iodide solutions containing no added organics) over a broad range of iodide and ozone concentrations, confirming previous results.[23,43,55,61] For the first time, this reduction in I_2 is demonstrated to be larger for surface microlayer samples than for subsurface seawater samples. Unfortunately, there are very few observations of ambient open-ocean I_2 with which to compare our results. Lawler et al.[61] inferred an I_2 flux around 2.0×10^7 molecules cm^{-2} s^{-1} from measurements of night-time I_2 at Cape Verde ($[O_3]$ = 25 to 45 ppbv); however, the same paper invoked range of I_2 fluxes 7×10^6 molecules cm^{-2} s^{-1} to 8.7×10^7 molecules cm^{-2} s^{-1} to model the diurnal cycles observed for I_2 and IO. Under similar conditions ($[O_3]$ = 38.5 ppbv, assuming oceanic $[I^-] = 1.5 \times 10^{-7}$ M), the interfacial model constrained by our present measurements gives I_2 fluxes of 5.5×10^6 molecules cm^{-2} s^{-1} for SSW and 1.4×10^6 molecules cm^{-2} s^{-1} for SML (extrapolated lines in Figure 4). Although our SML result is clearly lower, our SSW result is close to the lowest I_2 fluxes considered by Lawler et al. Interestingly, our SML result agrees well with the I_2 fluxes (1.4 to 2.5×10^6 molecules cm^{-2} s^{-1}) reported from the early laboratory study of Garland and Curtis[23] on natural seawater "from the Dorset coast, U.K." (assumed $[I^-]$ = 12.5 μg dm^{-3} = 1.0×10^{-7} M, $[O_3]$ = 35 ppbv).

The presence of organics in natural seawater resulted in a very small flux of halocarbons, mainly CH_3I, formed from chemistry subsequent to the surface reaction of ozone. The interfacial model predicts that the VOI flux makes its biggest relative contribution to the total iodine flux at low iodide concentrations (red line Figure S6), nevertheless the VOI emissions remain a negligible fraction (<5%) of the total iodine (VOI + 2 × I_2 + HOI) emissions for iodide concentrations relevant to environmental conditions.

We show that the observed reduction of I_2 emissions is likely to be due to the increased solubility of I_2 in the organic-enriched seawater (compared to artificial seawater or buffered KI solutions). Our results are consistent with the solubility of I_2 being a factor of 6 higher in SSW and ×30 higher in SML, compared to pure water. We calculated enrichment factors (EF), defined as the ratio of the SML over the SSW, based on the concentration of [DOC] ($EF_{[DOC]}$) or on the surface pressure (EF_π). These can be used as an indication of the enrichment at the surface (see sections 1.4 & 1.5 of the SI and Table S2). The $EF_{[DOC]}$ = 0.9 to 2.3 does not reflect the inferred factor of 5 difference in I_2 solubility between the SML and SSW. However, this difference in solubility does fall in the range of EF_π = 4.3 to 8.1 and hence seems more related to changes in the surface tension. More data are needed to confirm this relationship. This solubility effect may not result in reduced HOI emissions and may even lead to enhanced HOI emissions from organic-enriched seawater because HOI is very water-soluble. Experiments are highly desirable to confirm or otherwise this hypothesis.

ASSOCIATED CONTENT

Supporting Information

The Supporting Information is available free of charge at https://pubs.acs.org/doi/10.1021/acs.est.0c02736.

> Material and methods; literature overview of the influence of organics on iodine (I_2) emissions (Table S1); overview of sample locations and times for the natural seawater samples (Table S2); quantifier, qualifier, and retention times used in the GC analysis of halocarbons (Table S3); experimental setup for the molecular iodine (I_2) measurements by broadband cavity enhanced absorption (BBCEAS) (Figure S1); experimental setup for the halocarbon measurements (Figure S2); comparison of observed iodine fluxes for samples of different dates (Figure S3); observed and modelled iodine fluxes over artificial solutions (Figure S4); observed and modelled iodine fluxes over natural

samples (Figure S5); relative contribution of simulated VOI emissions (Figure S6) (PDF)

AUTHOR INFORMATION

Corresponding Author

Liselotte Tinel − *Department of Chemistry, University of York, York YO10 5DD, U.K.*; orcid.org/0000-0003-1742-2755; Email: liselotte.tinel@york.ac.uk

Authors

Thomas J. Adams − *School of Chemistry, University of Leicester, Leicester LE1 7RH, U.K.; Ricardo Energy & Environment, Oxfordshire OX11 0QR, U.K.*

Lloyd D. J. Hollis − *School of Chemistry, University of Leicester, Leicester LE1 7RH, U.K.*; orcid.org/0000-0001-7689-1565

Alice J. M. Bridger − *School of Chemistry, University of Leicester, Leicester LE1 7RH, U.K.*

Rosie J. Chance − *Department of Chemistry, University of York, York YO10 5DD, U.K.*; orcid.org/0000-0002-5906-176X

Martyn W. Ward − *Department of Chemistry, University of York, York YO10 5DD, U.K.*

Stephen M. Ball − *School of Chemistry, University of Leicester, Leicester LE1 7RH, U.K.*

Lucy J. Carpenter − *Department of Chemistry, University of York, York YO10 5DD, U.K.*; orcid.org/0000-0002-6257-3950

Complete contact information is available at: https://pubs.acs.org/10.1021/acs.est.0c02736

Notes

The authors declare no competing financial interest.

ACKNOWLEDGMENTS

This work was funded by the Natural Environment Research Council (NERC), U.K., through the grant "Iodide in the ocean: distribution and impact on iodine flux and ozone loss" (NE/N009983/1 University of York and NE/N009444/1 University of Leicester). L.J.C. also acknowledges funding from the European Research Council (ERC) under the European Union's Horizon 2020 program (Grant agreement No. 833290).

REFERENCES

(1) Stone, D.; Sherwen, T.; Evans, M. J.; Vaughan, S.; Ingham, T.; Whalley, L. K.; Edwards, P. M.; Read, K. A.; Lee, J. D.; Moller, S. J.; Carpenter, L. J.; Lewis, A. C.; Heard, D. E. Impacts of Bromine and Iodine Chemistry on Tropospheric OH and HO2: Comparing Observations with Box and Global Model Perspectives. *Atmos. Chem. Phys.* **2018**, *18*, 3541−3561.

(2) Sherwen, T.; Evans, M. J.; Carpenter, L. J.; Andrews, S. J.; Lidster, R. T.; Dix, B.; Koenig, T. K.; Sinreich, R.; Ortega, I.; Volkamer, R.; Saiz-Lopez, A.; Prados-Roman, C.; Mahajan, A. S.; Ordóñez, C. Iodine's Impact on Tropospheric Oxidants: A Global Model Study in GEOS-Chem. *Atmos. Chem. Phys.* **2016**, *16*, 1161−1186.

(3) Badia, A.; Reeves, C. E.; Baker, A. R.; Saiz-Lopez, A.; Volkamer, R.; Koenig, T. K.; Apel, E. C.; Hornbrook, R. S.; Carpenter, L. J.; Andrews, S. J.; Sherwen, T.; von Glasow, R. Importance of Reactive Halogens in the Tropical Marine Atmosphere: A Regional Modelling Study Using WRF-Chem. *Atmos. Chem. Phys.* **2019**, *19*, 3161−3189.

(4) Sarwar, G.; Gantt, B.; Foley, K.; Fahey, K.; Spero, T. L.; Kang, D.; Mathur, R.; Foroutan, H.; Xing, J.; Sherwen, T.; Saiz-Lopez, A. Influence of Bromine and Iodine Chemistry on Annual, Seasonal, Diurnal, and Background Ozone: CMAQ Simulations over the Northern Hemisphere. *Atmos. Environ.* **2019**, *213*, 395−404.

(5) Sherwen, T.; Evans, M. J.; Carpenter, L. J.; Schmidt, J. A.; Mickley, L. J. Halogen Chemistry Reduces Tropospheric O3 Radiative Forcing. *Atmos. Chem. Phys.* **2017**, *17*, 1557−1569.

(6) Ganzeveld, L.; Helmig, D.; Fairall, C. W.; Hare, J.; Pozzer, A. Atmosphere-Ocean Ozone Exchange: A Global Modeling Study of Biogeochemical, Atmospheric, and Waterside Turbulence Dependencies. *Global Biogeochem. Cycles* **2009**, *23*, 1−16.

(7) Gantt, B.; Sarwar, G.; Xing, J.; Simon, H.; Schwede, D.; Hutzell, W. T.; Mathur, R.; Saiz-Lopez, A. The Impact of Iodide-Mediated Ozone Deposition and Halogen Chemistry on Surface Ozone Concentrations Across the Continental United States. *Environ. Sci. Technol.* **2017**, *51*, 1458−1466.

(8) Koenig, T. K.; Baidar, S.; Campuzano-Jost, P.; Cuevas, C. A.; Dix, B.; Fernandez, R. P.; Guo, H.; Hall, S. R.; Kinnison, D.; Nault, B. A.; Ullmann, K.; Jimenez, J. L.; Saiz-Lopez, A.; Volkamer, R. Quantitative Detection of Iodine in the Stratosphere. *Proc. Natl. Acad. Sci. U.S.A.* **2020**, *117*, 1860−1866.

(9) Chameides, W. L.; Davis, D. D. Iodine: Its Possible Role in Tropospheric Photochemistry. *J. Geophys. Res.* **1980**, *85*, 7383−7398.

(10) Read, K. A.; Mahajan, A. S.; Carpenter, L. J.; Evans, M. J.; Faria, B. V. E.; Heard, D. E.; Hopkins, J. R.; Lee, J. D.; Moller, S. J.; Lewis, A. C.; Mendes, L.; McQuaid, J. B.; Oetjen, H.; Saiz-Lopez, A.; Pilling, M. J.; Plane, J. M. C. Extensive Halogen-Mediated Ozone Destruction over the Tropical Atlantic Ocean. *Nature* **2008**, *453*, 1232−1235.

(11) Kasibhatla, P.; Sherwen, T.; Evans, M. J.; Carpenter, L. J.; Reed, C.; Alexander, B.; Chen, Q.; Sulprizio, M. P.; Lee, J. D.; Read, K. A.; Bloss, W.; Crilley, L. R.; Keene, W. C.; Pszenny, A. A. P.; Hodzic, A. Global Impact of Nitrate Photolysis in Sea-Salt Aerosol on NOx, OH, and O3 in the Marine Boundary Layer. *Atmos. Chem. Phys.* **2018**, *18*, 11185−11203.

(12) Mahajan, A. S.; Oetjen, H.; Saiz-Lopez, A.; Lee, J. D.; McFiggans, G. B.; Plane, J. M. C. Reactive Iodine Species in a Semi-Polluted Environment. *Geophys. Res. Lett.* **2009**, *36*, No. L16803.

(13) McFiggans, G.; Bale, C. S. E.; Ball, S. M.; Beames, J. M.; Bloss, W. J.; Carpenter, L. J.; Dorsey, J.; Dunk, R.; Flynn, M. J.; Furneaux, K. L.; Gallagher, M. W.; Heard, D. E.; Hollingsworth, A. M.; Hornsby, K.; Ingham, T.; Jones, C. E.; Jones, R. L.; Kramer, L. J.; Langridge, J. M.; Leblanc, C.; LeCrane, J.-P.; Lee, J. D.; Leigh, R. J.; Longley, I.; Mahajan, A. S.; Monks, P. S.; Oetjen, H.; Orr-Ewing, A. J.; Plane, J. M. C.; Potin, P.; Shillings, A. J. L.; Thomas, F.; von Glasow, R.; Wada, R.; Whalley, L. K.; Whitehead, J. D. Iodine-Mediated Coastal Particle Formation: An Overview of the Reactive Halogens in the Marine Boundary Layer (RHaMBLe) Roscoff Coastal Study. *Atmos. Chem. Phys.* **2010**, *10*, 2975−2999.

(14) Dall'Osto, M.; Simo, R.; Harrison, R. M.; Beddows, D. C. S.; Saiz-Lopez, A.; Lange, R.; Skov, H.; Nøjgaard, J. K.; Nielsen, I. E.; Massling, A. Abiotic and Biotic Sources Influencing Spring New Particle Formation in North East Greenland. *Atmos. Environ.* **2018**, *190*, 126−134.

(15) Cuevas, C. A.; Maffezzoli, N.; Corella, J. P.; Spolaor, A.; Vallelonga, P.; Kjær, H. A.; Simonsen, M.; Winstrup, M.; Vinther, B.; Horvat, C.; Fernandez, R. P.; Kinnison, D.; Lamarque, J.-F.; Barbante, C.; Saiz-Lopez, A. Rapid Increase in Atmospheric Iodine Levels in the North Atlantic since the Mid-20th Century. *Nat. Commun.* **2018**, *9*, No. 1452.

(16) Legrand, M.; McConnell, J. R.; Preunkert, S.; Arienzo, M.; Chellman, N.; Gleason, K.; Sherwen, T.; Evans, M. J.; Carpenter, L. J. Alpine Ice Evidence of a Three-Fold Increase in Atmospheric Iodine Deposition since 1950 in Europe Due to Increasing Oceanic Emissions. *Proc. Natl. Acad. Sci. U.S.A.* **2018**, *115*, 12136−12141.

(17) Saiz-Lopez, A.; Plane, J. M. C. Novel Iodine Chemistry in the Marine Boundary Layer. *Geophys. Res. Lett* **2004**, *31*, No. L04112.

(18) Mahajan, A. S.; Sorribas, M.; Martín, J. C. G.; MacDonald, S. M.; Gil, M.; Plane, J. M. C.; Saiz-Lopez, A. Concurrent Observations of Atomic Iodine, Molecular Iodine and Ultrafine Particles in a Coastal Environment. *Atmos. Chem. Phys.* **2011**, *11*, 2545−2555.

https://dx.doi.org/10.1021/acs.est.0c02736
Environ. Sci. Technol. 2020, 54, 13228−13237

(19) Carpenter, L. J.; MacDonald, S. M.; Shaw, M. D.; Kumar, R.; Saunders, R. W.; Parthipan, R.; Wilson, J.; Plane, J. M. C. Atmospheric Iodine Levels Influenced by Sea Surface Emissions of Inorganic Iodine. *Nat. Geosci.* **2013**, *6*, 108−111.
(20) Prados-Roman, C.; Cuevas, C. A.; Hay, T.; Fernandez, R. P.; Mahajan, A. S.; Royer, S.-J.; Galí, M.; Simó, R.; Dachs, J.; Großmann, K.; Kinnison, D. E.; Lamarque, J.-F.; Saiz-Lopez, A. Iodine Oxide in the Global Marine Boundary Layer. *Atmos. Chem. Phys.* **2015**, *15*, 583−593.
(21) Ullman, W. J.; Luther, G. W.; De Lange, G. J.; Woittiez, J. R. W. Iodine Chemistry in Deep Anoxic Basins and Overlying Waters of the Mediterranean Sea. *Mar. Chem.* **1990**, *31*, 153−170.
(22) Farrenkopf, A. M.; Luther, G. W., III Iodine Chemistry Reflects Productivity and Denitrification in the Arabian Sea: Evidence for Flux of Dissolved Species from Sediments of Western India into the OMZ. *Deep Sea Res., Part II* **2002**, *49*, 2303−2318.
(23) Garland, J. A.; Curtis, H. Emission of Iodine from the Sea Surface in the Presence of Ozone. *J. Geophys. Res.* **1981**, *86*, 3183.
(24) Sakamoto, Y.; Yabushita, A.; Kawasaki, M.; Enami, S. Direct Emission of I2 Molecule and IO Radical from the Heterogeneous Reactions of Gaseous Ozone with Aqueous Potassium Iodide Solution. *J. Phys. Chem. A* **2009**, *113*, 7707−7713.
(25) Chance, R. J.; Tinel, L.; Sherwen, T.; Baker, A. R.; Bell, T.; Brindle, J.; Campos, M. L. A. M.; Croot, P.; Ducklow, H.; Peng, H.; Hopkins, F.; Hoogakker, B.; Hughes, C.; Jickells, T. D.; Loades, D.; Macaya, D. A. R.; Mahajan, A. S.; Malin, G.; Phillips, D.; Roberts, I.; Roy, R.; Sarkar, A.; Sinha, A. K.; Song, X.; Winkelbauer, H.; Wuttig, K.; Yang, M.; Peng, Z.; Carpenter, L. J. Global Sea-Surface Iodide Observations, 1967−2018. *Sci. Data* **2019**, *6*, 286.
(26) Inamdar, S.; Tinel, L.; Chance, R.; Carpenter, L. J.; Sabu, P.; Chacko, R.; Tripathy, S. C.; Kerkar, A. U.; Sinha, A. K.; Bhaskar, P. V.; Sarkar, A.; Roy, R.; Sherwen, T.; Cuevas, C.; Saiz-Lopez, A.; Ram, K.; Mahajan, A. S. Estimation of Reactive Inorganic Iodine Fluxes in the Indian and Southern Ocean Marine Boundary Layer. *Atmos. Chem. Phys. Discuss* **2020**, *2020*, 1−57.
(27) Magi, L.; Schweitzer, F.; Pallares, C.; Cherif, S.; Mirabel, P.; George, C. Investigation of the Uptake Rate of Ozone and Methyl Hydroperoxide by Water Surfaces. *J. Phys. Chem. A* **1997**, *101*, 4943−4949.
(28) Haag, W. R.; Hoigné, J. Kinetics and Products of the Reactions of Ozone with Various Forms of Chlorine and Bromine in Water. *Ozone: Sci. Eng.* **1984**, *6*, 103−114.
(29) Haruta, K.; Takeyama, T. Kinetics of Oxidation of Aqueous Bromide Ion by Ozone. *J. Phys. Chem. A* **1981**, *85*, 2383−2388.
(30) Harvey, H. W. The Chemistry and Fertility of Sea Waters, H. W. Harvey, Sc.D., F.R.S. Cambridge: Cambridge University Press, 1955. *J. Mar. Biol. Assoc.* **1956**, *35*, 289.
(31) Jungwirth, P.; Tobias, D. J. Molecular Structure of Salt Solutions: A New View of the Interface with Implications for Heterogeneous Atmospheric Chemistry. *J. Phys. Chem. B* **2001**, *105*, 10468−10472.
(32) Gladich, I.; Shepson, P. B.; Carignano, M. A.; Szleifer, I. Halide Affinity for the Water−Air Interface in Aqueous Solutions of Mixtures of Sodium Salts. *J. Phys. Chem. A* **2011**, *115*, 5895−5899.
(33) Moreno, C. G.; Gálvez, O.; López-Arza Moreno, V.; Espildora-García, E. M.; Baeza-Romero, M. T. A Revisit of the Interaction of Gaseous Ozone with Aqueous Iodide. Estimating the Contributions of the Surface and Bulk Reactions. *Phys. Chem. Chem. Phys.* **2018**, *20*, 27571−27584.
(34) van Pinxteren, M.; Müller, C.; Iinuma, Y.; Stolle, C.; Herrmann, H. Chemical Characterization of Dissolved Organic Compounds from Coastal Sea Surface Microlayers (Baltic Sea, Germany). *Environ. Sci. Technol.* **2012**, *46*, 10455−10462.
(35) Kuznetsova, M.; Lee, C.; Aller, J.; Frew, N. Enrichment of Amino Acids in the Sea Surface Microlayer at Coastal and Open Ocean Sites in the North Atlantic Ocean. *Limnol. Oceanogr.* **2004**, *49*, 1605−1619.
(36) Schmidt, R.; Schneider, B. The Effect of Surface Films on the Air−Sea Gas Exchange in the Baltic Sea. *Mar. Chem.* **2011**, *126*, 56−62.
(37) Kock, A.; Schafstall, J.; Dengler, M.; Brandt, P.; Bange, H. W. Sea-to-Air and Diapycnal Nitrous Oxide Fluxes in the Eastern Tropical North Atlantic Ocean. *Biogeosciences* **2012**, *9*, 957−964.
(38) Engel, A.; Bange, H. W.; Cunliffe, M.; Burrows, S. M.; Friedrichs, G.; Galgani, L.; Herrmann, H.; Hertkorn, N.; Johnson, M.; Liss, P. S.; Quinn, P. K.; Schartau, M.; Soloviev, A.; Stolle, C.; Upstill-Goddard, R. C.; van Pinxteren, M.; Zäncker, B. The Ocean's Vital Skin: Toward an Integrated Understanding of the Sea Surface Microlayer. *Front. Mar. Sci.* **2017**, *4*, 165.
(39) Carpenter, L. J.; Nightingale, P. D. Chemistry and release of gases from the surface ocean. *Chem. Rev.* **2015**, 4015−4034.
(40) Reeser, D. I.; Donaldson, D. J. Influence of Water Surface Properties on the Heterogeneous Reaction between O3(g) and I(Aq)−. *Atmos. Environ.* **2011**, *45*, 6116−6120.
(41) Hayase, S.; Yabushita, A.; Kawasaki, M.; Enami, S.; Hoffmann, M. R.; Colussi, A. J. Weak Acids Enhance Halogen Activation on Atmospheric Water's Surfaces. *J. Phys. Chem. A* **2011**, *115*, 4935−4940.
(42) Hayase, S.; Yabushita, A.; Kawasaki, M.; Enami, S.; Hoffmann, M. R.; Colussi, A. J. Heterogeneous Reaction of Gaseous Ozone with Aqueous Iodide in the Presence of Aqueous Organic Species. *J. Phys. Chem. A* **2010**, *114*, 6016−6021.
(43) Shaw, M. D.; Carpenter, L. J. Modification of Ozone Deposition and I2 Emissions at the Air − Aqueous Interface by Dissolved Organic Carbon of Marine Origin. *Environ. Sci. Technol.* **2013**, *47*, 10947−10954.
(44) Martino, M.; Mills, G. P.; Woeltjen, J.; Liss, P. S. A New Source of Volatile Organoiodine Compounds in Surface Seawater. *Geophys. Res. Lett* **2009**, *36*, No. L01609.
(45) Ball, S. M.; Hollingsworth, A. M.; Humbles, J.; Leblanc, C.; Potin, P.; McFiggans, G. Spectroscopic Studies of Molecular Iodine Emitted into the Gas Phase by Seaweed. *Atmos. Chem. Phys.* **2010**, *10*, 6237−6254.
(46) Vikis, A. C.; MacFarlane, R. Reaction of Iodine with Ozone in the Gas Phase. *J. Phys. Chem. V* **1985**, *89*, 812−815.
(47) Johnson, M. T. A Numerical Scheme to Calculate Temperature and Salinity Dependent Air-Water Transfer Velocities for Any Gas. *Ocean Sci.* **2010**, *6*, 913−932.
(48) Weisenberger, S.; Schumpe, A. Estimation of Gas Solubilities in Salt Solutions at Temperatures from 273 K to 363 K. *AIChE J.* **1996**, *42*, 298−300.
(49) Biń, A. Ozone Solubility in Liquids. *Ozone Sci. Eng.* **2006**, *28*, 67−75.
(50) Moreno, C.; Baeza-Romero, M. T. A Kinetic Model for Ozone Uptake by Solutions and Aqueous Particles Containing I- and Br-, Including Seawater and Sea-Salt Aerosol. *Phys. Chem. Chem. Phys.* **2019**, *21*, 19835−19856.
(51) Bichsel, Y.; Von Gunten, U. Oxidation of Iodide and Hypoiodous Acid in the Disinfection of Natural Waters. *Environ. Sci. Technol.* **1999**, *33*, 4040−4045.
(52) Keene, W. C.; Pszenny, A. A. P.; Jacob, D. J.; Duce, R. A.; Galloway, J. N.; Schultz-Tokos, J. J.; Sievering, H.; Boatman, J. F. The Geochemical Cycling of Reactive Chlorine through the Marine Troposphere. *Global Biogeochem. Cycles* **1990**, *4*, 407−430.
(53) Hunt, S. W.; Roeselová, M.; Wang, W.; Wingen, L. M.; Knipping, E. M.; Tobias, D. J.; Dabdub, D.; Finlayson-Pitts, B. J. Formation of Molecular Bromine from the Reaction of Ozone with Deliquesced NaBr Aerosol: Evidence for Interface Chemistry. *J. Phys. Chem. A* **2004**, *108*, 11559−11572.
(54) Truesdale, V. W.; Luther, G. W. Molecular Iodine Reduction by Natural and Model Organic Substances in Seawater. *Aquat. Geochem.* **1995**, *1*, 89−104.
(55) MacDonald, S. M.; Gómez Martín, J. C.; Chance, R.; Warriner, S.; Saiz-Lopez, A.; Carpenter, L. J.; Plane, J. M. C. A Laboratory Characterisation of Inorganic Iodine Emissions from the Sea Surface:

Dependence on Oceanic Variables and Parameterisation for Global Modelling. *Atmos. Chem. Phys.* **2014**, *14*, 5841−5852.
(56) De Barros Faria, R.; Lengyel, I.; Epstein, I. R.; Kustin, K. Systematic Design of Chemical Oscillators. 86. Combined Mechanism Explaining Nonlinear Dynamics in Bromine(III) and Bromine(V) Oxidations of Iodide Ion. *J. Phys. Chem. B* **1993**, *97*, 1164−1171.
(57) Weisenberger, S.; Schumpe, D. A. Estimation of Gas Solubilities in Salt Solutions at Temperatures from 273 K to 363 K. *AIChE J.* **1996**, *42*, 298−300.
(58) WHO. Guidelines for Drinking-Water Quality, Volume 2: Health Criteria and Other Supporting Information. *Sci. Total Environ.* **1987**, *61*, 274.
(59) Harner, T.; Shoeib, M. Measurements of Octanol-Air Partition Coefficients (KOA) for Polybrominated Diphenyl Ethers (PBDEs): Predicting Partitioning in the Environment. *J. Chem. Eng. Data* **2002**, *47*, 228−232.
(60) Bichsel, Y.; Von Gunten, U. Formation of Iodo-Trihalomethanes during Disinfection and Oxidation of Iodide-Containing Waters. *Environ. Sci. Technol.* **2000**, *34*, 2784−2791.
(61) Lawler, M. J.; Mahajan, A. S.; Saiz-Lopez, A.; Saltzman, E. S. Observations of I2 at a Remote Marine Site. *Atmos. Chem. Phys.* **2014**, *14*, 2669−2678.

https://dx.doi.org/10.1021/acs.est.0c02736
Environ. Sci. Technol. 2020, 54, 13228−13237